Modeling of the effect of the buried Si–SiO2 interface on transient enhanced boron diffusion in silicon on insulator

E. M Bazizi, P F Fazzini, A. Pakfar, C. Tavernier, B. Vandelle, H. Kheyrandish, S. Paul, W. Lerch, Fuccio Cristiano

Modeling of the effect of the buried Si–SiO_2 interface on transient enhanced boron diffusion in silicon on insulator

E. M. Bazizi,[1,2,3,a] P. F. Fazzini,[2,3] A. Pakfar,[1] C. Tavernier,[1] B. Vandelle,[1] H. Kheyrandish,[4] S. Paul,[5] W. Lerch,[5] and F. Cristiano[2,3]
[1]*STMicroelectronics, 850 rue Jean Monnet, 38926 Crolles Cedex, France*
[2]*CNRS-LAAS, 7 av. du col. Roche, 31077 Toulouse, France*
[3]*Université de Toulouse, UPS, INSA, INP, ISAE, LAAS, 31077 Toulouse, France*
[4]*CSMA-MATS, Stoke-on-Trent, Staffordshire ST4 7LQ, United Kingdom*
[5]*Mattson Thermal Products GmbH, Daimlerstr. 10, D-89160 Dornstadt, Germany*

(Received 5 November 2009; accepted 17 February 2010; published online 8 April 2010)

The effect of the buried Si–SiO_2 interface on the transient enhanced diffusion (TED) of boron in silicon on insulator (SOI) structures has been investigated. To this purpose, boron marker layers were grown by chemical vapor deposition on Si and SOI substrates and implanted under nonamorphizing conditions with 40 keV Si^+ ions. The experimental results clearly confirm that the Si–SiO_2 interface is an efficient trap for the Si interstitial atoms diffusing out of the defect region. Based on these experiments, existing models for the simulation of B TED in silicon have been modified to include an additional buried recombination site for silicon interstitials. The simulation results provide an upper limit of ~5 nm for the recombination length of interstitials at the Si–SiO_2 interface. © *2010 American Institute of Physics*. [doi:10.1063/1.3369160]

I. INTRODUCTION

The use of silicon on insulator (SOI) substrates provides significant advantages for the fabrication of future generations of electronic devices.[1] Reduced short channel effects, improved speed, and reduced power consumption in complementary metal oxide semiconductor devices are all achievable with these substrates.[2] An additional advantage of SOI consists of the possibility to reduce the number of silicon interstitials created during the source/drain implant steps by recombining them at the buried Si–SiO_2 interface, which results in a better control of several deleterious effects, such as extended defect formation,[3,4] dopant deactivation,[5] and transient enhanced diffusion (TED).[6]

The behavior of the buried Si–SiO_2 interface with respect to the implant-generated interstitial excess has been a longstanding subject of research and, with the exception of a few reports suggesting that the interface has no impact at all on dopant diffusion[7] or acts has a reflective boundary for interstitials,[8] the vast majority of previous reports shows that it behaves as an efficient sink for interstitials.[3–6,9–11] Several physical phenomena have been investigated in these studies which give a more or less direct evidence of the interstitial recombination at the Si–SiO_2 interface. In some cases, a quantitative estimation of the recombination length for interstitials at the interface L_{int} has also been given. However, one of these studies was based on the observation of the boron pileup at the Si–SiO_2 interface,[10] which is difficult to measure by secondary ion mass spectroscopy (SIMS) due to the change in sputtering and ionization rate at the interface. It does also strongly depend on the SOI fabrication method.[12] Others were based on the investigation of boron deactivation due to silicon interstitial atoms emitted by end-of-range defects.[5,11] This requires the concomitant use of structural and electrical measurements [transmission electron microscopy (TEM), SIMS, Hall effect], and several strong assumptions for their quantitative modeling.

Dopant diffusion studies, especially when based on *in situ* grown dopant marker layers, are expected to provide the most reliable estimation of L_{int}, as they only rely on SIMS measurements and dopant diffusion modeling. Indeed, these have been used in the past to show and quantify the interstitial recombination at the silicon surface (L_{surf}).[13–16] However, when applied to SOI, this method was mainly used to study oxidation-enhanced diffusion,[9] yielding L_{int} values (>1 μm above 800 °C) much larger than those proposed in SOI studies based on different methods ($L_{int}<10$ nm).[5,10,11]

In this work, we therefore investigate the effect of the buried Si–SiO_2 interface on the TED of boron marker layers grown on SOI substrates following a nonamorphizing implant. We show that this interface acts as an additional sink for interstitials during thermal anneal and provide a reliable estimation of the interface recombination length.

II. EXPERIMENTAL DETAILS

A reference bulk Cz–Si wafer and a Smart-Cut SOI wafer with a Si top layer thickness of 160 nm were used for this study. A chemical vapor deposition (CVD)-grown layer was then deposited on top of each wafer, with a thickness of ~1.5 μm and containing three boron marker layers with a peak concentration of $\sim 1\times 10^{18}$ cm^{-3}, located at a depth of 0.2, 0.8, and 1.3 μm in the Si wafer and a depth of 0.1, 0.6, and 1.0 μm in the SOI wafer. Implantation damage was then created in both wafers by a nonamorphizing Si^+ implant at 40 keV to a dose of 6×10^{13} cm^{-2}. The wafers were then cut into 2×2 cm^2 pieces and corresponding samples from each

[a]Author to whom correspondence should be addressed. Electronic mail: el-mehdi.bazizi-cnrs@st.com.

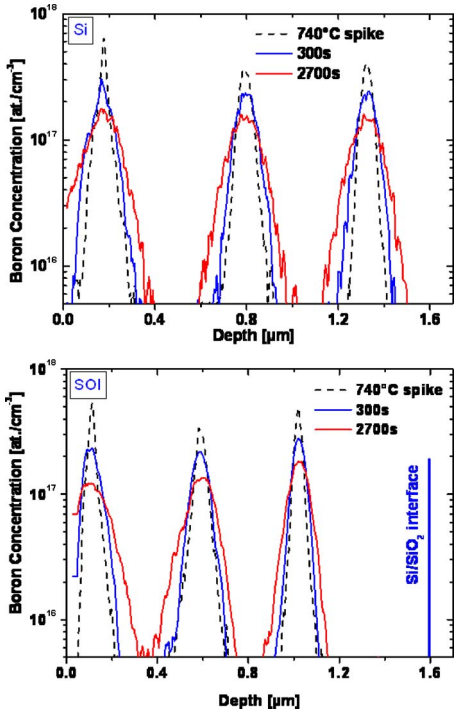

FIG. 1. (Color online) Boron depth distribution profiles in (a) Si and (b) SOI structures measured by SIMS following a 40 keV Si^+ implant to a dose of 6×10^{13} cm^{-2} and annealing at 740 °C for various time intervals.

one were simultaneously annealed at 740 °C in N_2 for times ranging from 1 s to 2 h, using a Mattson 3000 Plus RTP system equipped with Mattson's absolute temperature measurement and wafer rotation. In such conditions, an extended defects layer consisting of {311} defects is formed, with a defect density peak at a depth of ~100 nm[17] and an initial width of ~150 nm. The presence of a boron marker layer in the defect region is not expected to affect defect formation, due to the low boron concentration ($<1\times10^{18}$ cm^{-3}), i.e., the extrinsic defects created by the implant consist only of self-interstitial clusters, as previously reported in Ref. 18.

The boron chemical profiles were measured by SIMS using a CAMECA IMS 6F system with 1000 eV O_2 primary ions and oxygen flooding under non-roughening conditions.[19] The depth calibration was carried out using a stylus (Dektak) surface profiler to measure the SIMS crater depth. Selected samples were analyzed by TEM in a JEOL 2010-HC microscope, following a standard specimen preparation technique (mechanical and dimple grinding followed by PIPS ion milling). Weak beam dark field analysis[20] was used to measure defect density, size, and position. Finally, for the diffusion data analysis, we used a fitting method based on the interstitial kick-out mechanism[21] to extract the diffusion enhancement, D_B/D_B^*, which provides, in turn, a direct measurement of the silicon point defect supersaturation, $S_{int}=D_B/D_B^*=C_I/C_I^*$, where D_B is the bc8oron diffusivity, C_I is the interstitial point defects concentration, and the stars indicate the parameters' equilibrium values.

III. RESULTS AND DISCUSSION

Figure 1 shows B depth profiles measured by SIMS in the bulk Si reference [Fig. 1(a)] and in the SOI wafer [Fig. 1(b)] after implantation with 40 keV Si^+, 6×10^{13} cm^{-2}, and annealing at 740 °C for different times (1, 300, and 2700 s, respectively). A significant diffusive broadening is observed for all the boron marker layers after each time interval. This broadening largely exceeds what would be expected from an equilibrium diffusion process, indicating that implantation-induced enhanced diffusion has occurred, in agreement with the presence of a defect layer in the implanted region.[22] In addition, it appears that the three boron marker layers in the Si wafer exhibit similar diffusion behavior independent of their depth position. In contrast, the broadening of the marker layers in the SOI wafer, while being systematically less pronounced than in the Si reference, continuously decreases when going from the shallowest to the deepest one. These results are clearly consistent with an efficient interstitial trapping at the buried $Si-SiO_2$ interface, in agreement with previous reports.[6,10] However, a quantitative analysis of the experimental results can only be done after the TED levels associated to the measured profile broadenings have been correctly evaluated.

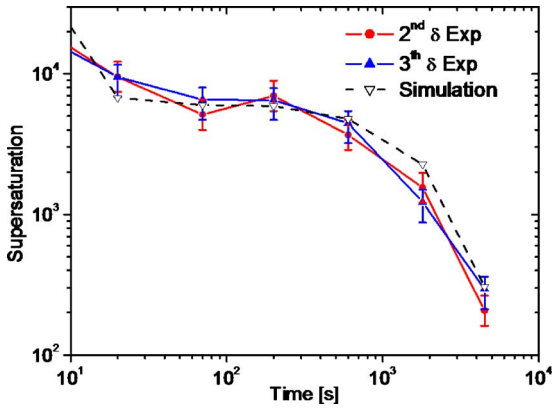

FIG. 2. (Color online) Time evolution of the interstitial supersaturation in the Si reference structure following a 40 keV Si^+ implant to a dose of 6×10^{13} cm^{-2} and annealing at 740 °C. Filled symbols and solid lines: measured values from boron marker layers located at a depth of 780 and 1330 nm. Empty symbols and dashed line: simulated values with Sprocess (surface recombination length L_{surf}: 1 nm).

For the TED evaluation, the shallowest marker layer in both wafers has not been considered, as they lie within the defect region (at 0.2 and 0.1 μm in the Si and SOI wafers, respectively); the diffusion of some of the boron atoms they contain might therefore be strongly affected by the vicinity of the surface. In contrast, considering the high diffusivity of silicon interstitials, the interstitial supersaturation measured from the two deepest marker layers contained in each wafer will reflect the one existing in the defect region and its depth variation will only depend on the eventual presence of bulk traps in the grown structures.

The results obtained for the reference Si wafer at an annealing temperature of 740 °C are shown in Fig. 2 (filled symbols and solid lines). The reported time evolution of the S_{int} is in agreement with the well known evolution of the implantation-induced defects responsible for the diffusion enhancement.[22,23] The almost constant value of supersaturation for annealing times up to 600 s corresponds to the Ostwald ripening of the {311} defects, while the final decrease is

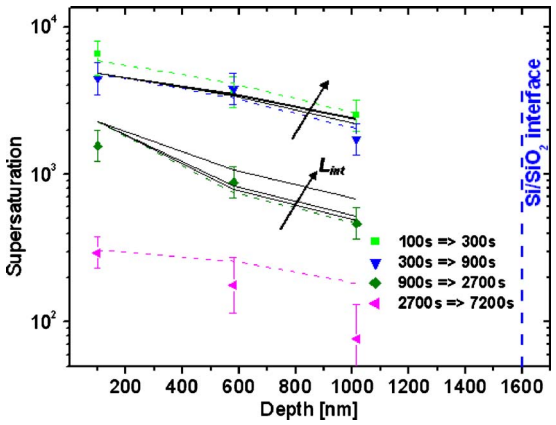

FIG. 3. (Color online) Depth dependence of the average diffusion enhancement (interstitial supersaturation) of boron marker layers grown on a SOI substrate, over different time intervals during annealing at 740 °C. Damage implant: 40 keV Si^+, 6×10^{13} cm^{-2}. Symbols: measured values. Color dashed lines: simulated values with Sprocess (interface recombination length L_{int}: 1 nm). Black solid lines: simulated values with increasing values of L_{int} (5, 10, and 40 nm; see arrows).

due to their dissolution. Such trend in the defect evolution has also been confirmed by TEM analysis of selected samples (not shown). More importantly, both boron marker layers exhibit the same diffusion enhancement, independently of their depth. Considering the high diffusivity of silicon interstitials and the absence of bulk traps in this wafer, the measured interstitial supersaturation therefore reflects the one existing in the defect region.

In Fig. 2, we also report the simulation results (empty symbols and dashed line) after annealing at 740 °C, obtained using the commercial software SENTAURUS PROCESS from Ref. 24. As-implanted interstitial and vacancy profiles are generated using the built-in implant simulator which is based on a Monte Carlo binary collision approximation model with cumulative damage. Boron diffusion is described by a five-stream diffusion model[24] already implemented in the process simulator. The whole defect evolution is described by the model of Zographos *et al.*,[25] based on the nonconservative Ostwald ripening mechanism, with the surface being a very efficient sink for silicon interstitial atoms diffusing out of the defect region (L_{surf}=1 nm). As shown in Fig. 2, after calibration, the time dependence of the interstitial supersaturation is perfectly predicted by the simulations.

The experimental results of boron TED in the SOI wafer are reported in Fig. 3 (symbols). In this figure, the interstitial supersaturation is plotted as a function of the depth of the analyzed marker layers and the various curves correspond to the different time intervals investigated. The points located at a depth of 100 nm represent the interstitial supersaturation value in the region containing the implantation-induced {311} defects, as extracted from the Si reference wafer, i.e., we assume that the defect evolution in the two wafers is identical. This hypothesis has been verified by TEM analysis (not shown). Indeed, due to the large distance between the defect region and the buried $Si-SiO_2$ interface (~1.5 μm), the defect dissolution in both wafers is entirely controlled by the proximity of the wafer surface (~100 nm). The experimental results shown in Fig. 3 clearly indicate that over the entire

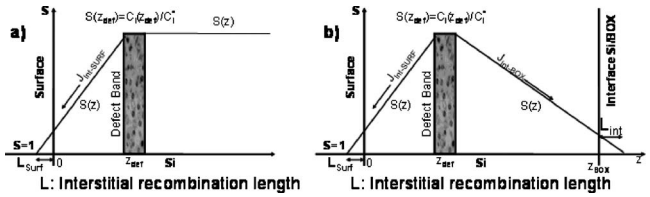

FIG. 4. Schematic representation of the loss of self interstitials toward the surface sink and the definition of the recombination length at the Si/BOX interface in SOI in the approximated model used in the simulations.

annealing time range, the interstitial supersaturation continuously decreases when approaching the buried $Si-SiO_2$ interface, confirming that excess interstitials diffusing out of the defect region recombine at the buried $Si-SiO_2$ interface, in agreement with previous studies.

In order to model the effect that the Si/BOX (buried oxide) interface can be considered as a strong sink for point defects, we have used the same assumption as for surface recombination. Indeed, the surface recombination is simulated using the first-order boundary conditions[26] assuming that the flux of interstitials is proportional to the excess of point defects [Fig. 4(a)] and that the annihilation of self-interstitials at kinks is diffusion limited.[27] The flux of interstitials at the surface is thus given by the following equation:

$$J_{int-surf} = D_I C_I^* S(z_{def})/(z_{def} + L_{surf}),$$

where $D_I C_I^*$ is the interstitial diffusivity, S is the interstitial supersaturation, z_{def} is the end of range (EOR) band position, and L_{surf} is the surface recombination length. To adapt this model to the case of SOI, we modify the equation describing the flux of interstitial toward the surface ($J_{int-surf}$). Assuming that the BOX interface also acts as a sink of interstitials but with a different recombination distance L_{int} we obtain the new flux toward the BOX

$$J_{int-BOX} = D_I C_I^* S(z_{def})/(z_{SOI} - z_{def} + L_{int}),$$

where z_{SOI} is the SOI thickness. A schematic picture of the fluxes and concentration variation in SOI structures is presented in Fig. 4(b).[28]

For the simulation of the SOI supersaturation data, the buried oxide layer is therefore placed below the Si CVD-grown layer, to account for the presence of an additional trapping interface, while keeping all other simulation parameters fixed to the values obtained from the reference Si wafer. Simulation results are shown in Fig. 3 (dashed lines). The recombination length for interstitials at the interface L_{int} was initially set at a value of 1 nm (i.e., same trapping efficiency as the silicon surface). With the exception of the longest annealing times, when the defects enter the dissolution stage (pink triangles in Fig. 3), the excellent agreement between simulations and experiments clearly confirms that the observed phenomenon in SOI wafers can be modeled in terms of an additional capture of interstitials at the buried $Si-SiO_2$ interface. The discrepancy between simulation and experiments for the 2700–7200 s time interval cannot be ascribed to a weakness of the defect simulation model, which was successfully used to simulate the whole defect evolution process in the reference Si wafer (cf. Fig. 2), but is probably due

to the increased difficulty in extracting a reliable interstitial supersaturation value in the late stages of TED, when the small observed profile broadening becomes comparable to the noise of the SIMS signal. Finally, simulations have been repeated using different values of L_{int} in order to assess the ability of this approach to provide a reliable estimation of the recombination efficiency. Results are reported in Fig. 3 for the time intervals 300–900s and 900–2700s (solid black lines) for increasing L_{int} values of 5, 10, and 40 nm, respectively, that correspond to progressively weaker recombination mechanisms. As expected, the simulated interstitial supersaturation in the defect region (located more than 1 μm away from the $Si-SiO_2$ interface) is insensitive to these variations in L_{int}. In contrast, in the vicinity of the interface, the supersaturation increases when increasing L_{int}. It is found that starting from a value of 10 nm, at least one of the experimental points is not correctly simulated. These results confirm that the $Si-SiO_2$ interface acts as a very efficient sink for silicon interstitials and provide an upper limit of ~ 5 nm for the interface recombination length.

IV. CONCLUSION

In summary, boron TED measurements were investigated using marker layers grown on Si and SOI wafers following a nonamorphizing implant. The obtained data clearly confirm that the $Si-SiO_2$ interface is an efficient trap for the Si interstitial atoms diffusing out of the defect region. Based on these experiments, existing models for the simulation of B TED in silicon have been modified to include an additional buried recombination site for silicon interstitials. The simulation results provide an upper limit of ~ 5 nm for the interface recombination length.

ACKNOWLEDGMENTS

This work has been carried out in the frame of the ATOMICS European Project (FP6, Contract No. 027152).

[1]International Roadmap for Semiconductor Technology, website: http://public.itrs.net.
[2]J. P. Colinge, *SOI Technology: Materials to VLSI*, 3rd ed. (Kluwer, Boston, 2004).
[3]A. F. Saavedra, K. S. Jones, M. E. Law, and K. K. Chan, Mater. Sci. Eng., B **107**, 198 (2004).
[4]P. F. Fazzini, F. Cristiano, C. Dupré, S. Paul, T. Ernst, H. Kheyrandish, K. K. Bourdelle, and W. Lerch, Mater. Sci. Eng., B **154–155**, 256 (2008).
[5]J. J. Hamilton, K. J. Kirkby, N. E. B. Cowern, E. J. H. Collart, M. Bersani, D. Giubertoni, S. Gennaro, and A. Parisini, Appl. Phys. Lett. **91**, 092122 (2007).
[6]J. J. Hamilton, N. E. B. Cowern, E. J. H. Collart, B. Colombeau, M. Bersani, D. Giubertoni, A. Parisini, J. A. Sharp, and K. J. Kirkby, Appl. Phys. Lett. **89**, 042111 (2006).
[7]K. L. Yeo, A. T. S. Wee, and Y. F. Chong, J. Appl. Phys. **96**, 3692 (2004).
[8]A. F. Saavedra, K. S. Jones, M. E. Law, K. K. Chan, and E. C. Jones, J. Appl. Phys. **96**, 1891 (2004).
[9]S. W. Crowder, C. J. Hsieh, P. B. Griffin, and J. D. Plummer, J. Appl. Phys. **76**, 2756 (1994).
[10]H.-H. Vuong, H.-J. Gossmann, L. Pelaz, G. K. Celler, D. C. Jacobson, D. Barr, J. Hergenrother, D. Monroe, V. C. Venezia, C. S. Rafferty, S. J. Hillenius, J. McKinley, F. A. Stevie, and C. Granger, Appl. Phys. Lett. **75**, 1083 (1999).
[11]K. R. C. Mok, B. Colombeau, M. Jaraiz, P. Castrillo, J. E. Rubio, R. Pinacho, M. P. Srinivasan, F. Benistant, I. Martin Bragado, and J. J. Hamilton, Mater. Res. Soc. Symp. Proc. **912**, C03.04 (2006).
[12]A. Ogura and M. Hiroi, Thin Solid Films **397**, 56 (2001).
[13]D. R. Lim, C. S. Rafferty, and F. P. Klemens, Appl. Phys. Lett. **67**, 2302 (1995).
[14]A. Agarwal, H.-J. Gossmann, D. J. Eaglesham, L. Pelaz, D. C. Jacobson, T. E. Haynes, and Yu. E. Erokhin, Appl. Phys. Lett. **71**, 3141 (1997).
[15]N. E. B. Cowern, D. Alquier, M. Omri, A. Claverie, and A. Nejim, Nucl. Instrum. Methods Phys. Res. B **148**, 257 (1999).
[16]Y. Lamrani, F. Cristiano, B. Colombeau, E. Scheid, P. Calvo, H. Schaefer, and A. Claverie, Nucl. Instrum. Methods Phys. Res. B **216**, 281 (2004).
[17]B. Colombeau, N. E. B. Cowern, F. Cristiano, P. Calvo, N. Cherkashin, Y. Lamrani, and A. Claverie, Appl. Phys. Lett. **83**, 1953 (2003).
[18]T. E. Haynes, D. J. Eaglesham, P. A. Stolk, H.-J. Gossmann, D. C. Jacobson, and J. M. Poate, Appl. Phys. Lett. **69**, 1376 (1996).
[19]C. W. Magee, G. R. Mount, S. P. Smith, B. Herner, and H.-J. Gossmann, J. Vac. Sci. Technol. B **16**, 3099 (1998).
[20]D. B. Williams and C. B. Carter, *Transmission Electron Microscopy: A Textbook for Materials Science* (Springer, New York, 1996).
[21]N. E. B. Cowern, K. T. F. Janssen, G. F. A. van de Walle, and D. J. Gravesteijn, Phys. Rev. Lett. **65**, 2434 (1990).
[22]N. E. B. Cowern, G. Mannino, P. A. Stolk, F. Roozeboom, H. G. A. Huizing, J. G. M. van Berkum, F. Cristiano, A. Claverie, and M. Jaraíz, Phys. Rev. Lett. **82**, 4460 (1999).
[23]A. Claverie, B. Colombeau, B. Mauduit, C. Bonafos, X. Herbras, G. Assayag, and F. Cristiano, Appl. Phys. A: Mater. Sci. Process. **76**, 1025 (2003).
[24]Sentaurus Process User Guide, Version Z-2007.03 (Synopsys Inc., Mountain 287 View, CA, 2007).
[25]N. Zographos, C. Zechner, and I. Avci, Mater. Res. Soc. Symp. Proc. **994**, F10 (2007).
[26]S. M. Hu, Appl. Phys. Lett. **27**, 165 (1975).
[27]S. M. Hu, Appl. Phys. Lett. **45**, 1567 (1974).
[28]P. F. Fazzini, F. Cristiano, C. Dupré, A. Claverie, T. Ernst, and M. Gavelle, J. Vac. Sci. Technol. B **26**, 342 (2008).